Interactions of intrinsically disordered *Thellungiella salsuginea* dehydrins TsDHN-1 and TsDHN-2 with membranes — synergistic effects of lipid composition and temperature on secondary structure

Luna N. Rahman, Lin Chen, Sumaiya Nazim, Vladimir V. Bamm, Mahmoud W. Yaish, Barbara A. Moffatt, John R. Dutcher, and George Harauz

Abstract: Dehydrins are intrinsically disordered (unstructured) proteins that are expressed in plants experiencing stressful conditions such as drought or low temperature. Dehydrins are typically found in the cytosol and nucleus, but also associate with chloroplasts, mitochondria, and the plasma membrane. Although their role is not completely understood, it has been suggested that they stabilize proteins or membrane structures during environmental stress, the latter association mediated by formation of amphipathic α-helices by conserved regions called the K-segments. *Thellungiella salsuginea* is a crucifer that thrives in the Canadian sub-Arctic (Yukon Territory) where it grows on saline-rich soils and experiences periods of both extreme cold and drought. We have cloned and expressed in *Escherichia coli* two dehydrins from this plant, denoted TsDHN-1 (acidic) and TsDHN-2 (basic). Here, we show using transmission-Fourier transform infrared (FTIR) spectroscopy that ordered secondary structure is induced and stabilized in these proteins by association with large unilamellar vesicles emulating the lipid compositions of plant plasma and organellar membranes. Moreover, this induced folding is enhanced at low temperatures, lending credence to the hypothesis that dehydrins stabilize plant outer and organellar membranes in conditions of cold.

Key words: dehydrins, late embryogenesis abundant (LEA), cold tolerance, intrinsically disordered protein (IDP), induced folding, CD spectroscopy, FTIR spectroscopy.

Résumé : Les déhydrines sont des protéines intrinsèquement désordonnées (non structurées) exprimées chez les plantes qui subissent des conditions de stress telles la sécheresse ou le froid. Les déhydrines sont typiquement trouvées dans le cytosol et le noyau, mais elles s'associent aussi aux chloroplastes, aux mitochondries et à la membrane plasmique. Même si leur rôle n'est pas complètement connu, il semble qu'elles stabiliseraient les protéines ou les structures membranaires lors d'un stress environnemental, cette dernière association étant réalisée par l'intermédiaire de la formation d'hélices-α amphipatiques dans les régions conservées appelées segments K. *Thellungiella salsuginea* est une crucifère qui prolifère dans les régions subarctiques du Canada (Territoire du Yukon), où il croit sur des sols riches en sels, étant soumis à des périodes de froid et de sécheresse extrêmes. Nous avons cloné et exprimé chez *Escherichia coli* deux déhydrines de cette plante, nommées TsDHN-1 (acide) et TsDHN-2 (basique). Nous montrons ici par spectroscopie de transmission infrarouge à trans-

Received 23 December 2009. Revision received 27 April 2010. Accepted 30 April 2010. Published on the NRC Research Press Web site at bcb.nrc.ca on 24 September 2010.

Abbreviations: CD, circular dichroism; Chol, cholesterol; TsDHN-1, acidic *Thellungiella salsuginea* dehydrin 1; TsDHN-2, basic *Thellungiella salsuginea* dehydrin 2; DGDG, digalactosyldiacylglycerol; FTIR, Fourier transform infrared; IDP, intrinsically disordered protein; LEA, late embryogenesis abundant; MARCKS, myristoylated alanine-rich C-kinase substrate; MGDG, monogalactosyldiacylglycerol; PC, phosphatidylcholine; PE, phosphatidylethanolamine; PG, phosphatidylglycerol; PI, phosphatidylinositol; PS, phosphatidylserine; SQDG, sulfoquinovosyl diacylglycerol.

L.N. Rahman, V.V. Bamm, and G. Harauz.[2] Department of Molecular and Cellular Biology, University of Guelph, Guelph, ON N1G 2W1, Canada; Biophysics Interdepartmental Group, University of Guelph, Guelph, ON N1G 2W1, Canada.
L. Chen. Department of Molecular and Cellular Biology, University of Guelph, Guelph, ON N1G 2W1, Canada; Department of Physics, University of Guelph, Guelph, ON N1G 2W1, Canada; Biophysics Interdepartmental Group, University of Guelph, Guelph, ON N1G 2W1, Canada.
S. Nazim and B.A. Moffatt. Department of Biology, University of Waterloo, Waterloo, ON N2L 3G1, Canada.
M.W. Yaish.[1] Department of Molecular and Cellular Biology, University of Guelph, Guelph, ON N1G 2W1, Canada; Department of Biology, University of Waterloo, Waterloo, ON N2L 3G1, Canada.
J.R. Dutcher. Department of Physics, University of Guelph, Guelph, ON N1G 2W1, Canada; Biophysics Interdepartmental Group, University of Guelph, Guelph, ON N1G 2W1, Canada.

[1]Present address: Department of Biology, College of Science, Sultan Qaboos University, 123 Muscat, P.O. Box 36, Oman.
[2]Corresponding author (e-mail: gharauz@uoguelph.ca).

formée de Fourier qu'une structure secondaire ordonnée est induite et stabilisée chez ces protéines par leur association à de larges vésicules monofeuillet imitant la composition en lipides des membranes plasmiques et des organelles. De plus, le repliement induit est augmenté à faible température, donnant crédit à l'hypothèse que les déhydrines stabilisent les membranes externes et les organelles des plantes au froid.

Mots-clés : déhydrines, LEA (late embryogenesis abundant), tolérance au froid, protéines intrinsèquement désordonnées, repliement induit, spectroscopie DC, spectroscopie FTIR.

[Traduit par la Rédaction]

Introduction

Plants have evolved many ways to cope with environmental stresses such as low temperature and drought. One response to these conditions is the induction of genes that encode the late embryogenesis abundant (LEA) proteins (Battaglia et al. 2008; Caramelo and Iusem 2009; Hundertmark and Hincha 2008). The way in which LEAs protect plants from environmental stress is not completely understood, although numerous mechanisms have been described (Wise and Tunnacliffe 2004; Rajesh and Manickam 2006; Tunnacliffe and Wise 2007; Battaglia et al. 2008). Among many macromolecular associations, LEAs have been suggested to stabilize plasma and organellar membranes (Hincha et al. 1990; Han et al. 1997; Danyluk et al. 1998; Steponkus et al. 1998; Ismail et al. 1999; Puhakainen et al. 2004; Beck et al. 2007; Tolleter et al. 2007; Zhang et al. 2010).

Most LEAs have also been recognized to be intrinsically disordered proteins (IDPs) (Eom et al. 1996; Lisse et al. 1996; Soulages et al. 2003; Mouillon et al. 2006; Goldgur et al. 2007; Hundertmark and Hincha 2008). Such proteins constitute roughly a third of the eukaryotic proteome and do not attain a defined tertiary fold, but adopt a specific conformation in association with other molecules (Uversky and Dunker 2010). It is generally considered that the intrinsically disordered and extended nature of LEAs imparts upon them the property of sequestering water and sugars in a tightly hydrogen-bonded network to form a hydrocolloid or gel (Hoekstra et al. 2001; Wolkers et al. 2001; Tompa et al. 2006; Kovacs et al. 2008; Shimizu et al. 2010). For example, cold and dehydration tolerance may depend in part on the amount of starch accumulation in the cell, as a source of protective di- and mono-saccharides (Maruyama et al. 2009). An important factor for starch degradation is the maintenance of α-amylase, and it has been suggested that LEAs preserve sufficient local water concentration to maintain α-amylase activity (Rinne et al. 1999).

At least six different groups of LEAs have been defined based on expression patterns and sequence (Wise and Tunnacliffe 2004; Tunnacliffe and Wise 2007; Battaglia et al. 2008; Hundertmark and Hincha 2008). The group 2 LEA proteins, also known as dehydrins, have been among the most widely studied (Campbell and Close 1997; Close 1997; Garay-Arroyo et al. 2000; Zhu et al. 2000; Allagulova et al. 2003; Puhakainen et al. 2004; Mouillon et al. 2006; Beck et al. 2007; Kosová et al. 2007, 2008 Battaglia et al. 2008). These proteins are generally enriched in glycyl and lysyl residues, but lack cysteinyl and tryptophanyl residues. Several hundred dehydrins have been purified from different sources; they range in size from ~5 to >200 kDa, and they contain three conserved sequences: the K-segment, the S-segment, and the Y-segment (Jepson and Close 1995; Campbell and Close 1997; Close 1997; Allagulova et al. 2003; Battaglia et al. 2008). The K-segment (consensus sequence EKKGIMDKIKEKLPG) is a lysine-rich domain that has the potential for electrostatic and hydrophobic interactions with membranes attributed to the formation of amphipathic α-helices (Campbell and Close 1997; Close 1997; Allagulova et al. 2003; Bravo et al. 2003; Koag et al. 2003, 2009; Rorat et al. 2006). The number of K-segments has been suggested as important in defining the degree of membrane association and putative stabilization (Bravo et al. 2003). The S-segment is a serine-rich domain that may be phosphorylated, modulating the dehydrin's ability to bind ligands such as divalent cationic metal ions (Heyen et al. 2002; Alsheikh et al. 2003; Zhang et al. 2006; Xu et al. 2008). The Y-segment (consensus sequence (V/T)DEYGNP) is found at the N-terminus, and is similar to the nucleotide-binding sites of plant and bacterial chaperone proteins. Dehydrins fall into one of five classes (K_n, SK_n, K_nS, Y_nSK_2, and Y_2K_n) based on their combination of K, S, and Y segments (Campbell and Close 1997; Close 1997; Allagulova et al. 2003; Battaglia et al. 2007).

Dehydrins are typically found in the cytoplasm and nucleus, but are also associated with the plasma membrane (Danyluk et al. 1998; Carjuzaa et al. 2008), or with chloroplasts or mitochondria (Hincha et al. 1990; Tolleter et al. 2007). Dehydrins form highly stable hydrated gels in vivo to sequester water (Wolkers et al. 2001; Tompa et al. 2006; Mouillon et al. 2008). Often (but not always), dehydrins gain ordered secondary structure upon interaction with detergents or lipids (Ceccardi et al. 1994; Ismail et al. 1999; Soulages et al. 2002; Koag et al. 2003, 2009; Soulages et al. 2003; Kovacs et al. 2008). In particular, the K-segment forms an amphipathic α-helix that can associate with membrane surfaces (Allagulova et al. 2003; Rorat et al. 2006).

Thellungiella salsuginea (also called *Thellungiella halophila*) has been proposed as a valuable new model plant for research on abiotic stress tolerance (Griffith et al. 2007; Amtmann 2009; Pedras and Zheng 2010). Here, we investigate the interactions of two *Thellungiella* dehydrins (denoted TsDHN-1 and TsDHN-2) with membranes as a function of temperature. Using circular dichroism (CD) and transmission-Fourier transform infrared (FTIR) spectroscopy, we demonstrate that membrane association increases the proportion of ordered secondary structure in each protein (induced folding), that the secondary structure composition depends on lipid type, and that low temperatures increase the degree of order of each dehydrin. These results support

the hypothesis that dehydrins stabilize plant outer and organellar membranes at low temperature.

Materials and methods

Materials

Most chemicals were reagent grade and acquired from either Fisher Scientific (Unionville, Ont.) or Sigma-Aldrich (Oakville, Ont.). Electrophoresis-grade chemicals were purchased from ICN Biomedicals (Costa Mesa, Calif.) or Bio-Rad Laboratories (Mississauga, Ont.). The Ni^{2+}–NTA (nitrilotriacetic acid) agarose beads were purchased from Qiagen (Mississauga, Ont.). Heavy water (D_2O) was obtained from Cambridge Isotope Laboratories (CIL, Andover, Mass.). The lipids phosphatidylcholine (PC), phosphatidylethanolamine (PE), phosphatidylglycerol (PG), phosphatidylinositol (PI), phosphatidylserine (PS), and cholesterol (Chol) were obtained from Avanti Polar Lipids (Alabaster, Ala.). The lipids digalactosyldiacylglycerol (DGDG), monogalactosyldiacylglycerol (MGDG), and sulfonoquinovosyl diacylglycerol (SQDG) were obtained from Lipid Products (Nutfield Nurseries, Redhill, Surrey, UK).

Recombinant dehydrin over-expression and purification

The open reading frames of the *Thellungiella* dehydrins designated TsDHN-1 and TsDHN-2 were amplified by PCR using the following forward (F) and reverse (R) primer pairs: CLDPTF (5′-GGAATTCCATATGGCGGAAGAGTACAAGAACG-3′) and CLDPTR (5′-TCCCCCGGGAGCATCAGACTCTTTTTC-3′), and INTDRTGF (5′-GGAATTCCATATGGCGTCTTACCAGAACCG-3′) and NTDRTGR (5′-ACGACCACCACCACCAGGAAGTTTATCTTTG-3′), respectively. Subsequently, the open reading frames of these *Thellungiella* dehydrins (designated TsDHN-1 and TsDHN-2, GenBank accession Nos. 1347304 and DN776754.1, respectively) were cloned as *Nde*I–*Sma*I fragments into the vector pTYB2 (New England Biolabs) and transformed into *Escherichia coli* DH5α cells.

The sequence-verified clones were introduced into *E. coli* ER2566 cells for over-expression. All cultures were grown at 37 °C in 2× YT (yeast–tryptone) media at pH 7.3 to OD_{600} = 0.8, at which time they were shifted to 30 °C and dehydrin expression was induced for 4 h by the addition of 0.1 mmol·L^{-1} isopropyl β-D-1-thiogalactopyranoside (IPTG).

Large-scale production of recombinant TsDHN-1 and TsDHN-2 was performed in fermentors at the Biotechnology Research Institute in Montréal, Que. For large-scale protein productions, batch fermentations were performed. A colony was selected from the plate for an overnight inoculation in 2× YT media. The overnight culture was then diluted 20-fold to inoculate 15 L of 2× YT media containing ampicillin in a 20 L bioreactor. The culture was grown at 37 °C until OD_{600} = 3, at which point expression was induced by 0.1 mmol·L^{-1} IPTG. The cells were grown for an additional 4 h at 30 °C before being harvested by centrifugation at 4000 r·min^{-1} (2831*g*) and a temperature of 4 °C. Since TsDHN-2 expressed significantly better in the batch fermentor in the absence of glucose, glucose was not added. However, to avoid the possibility of bacteria entering the stationary phase at an early stage, the cells were induced at a low OD_{600}.

Purification was performed using IMPACT affinity chromatography following the manufacturer's instructions (New England Biolabs 2010) and a previously published protocol (Chong et al. 1997). This system does not require a protease for the affinity tag removal. Instead, either dithiothreitol (DTT), β-mercaptoethanol, or cysteine can induce the intein to self-cleave, thus releasing the target protein from the chitin-bound intein tag.

An additional step of ion exchange chromatography on either HiTrap™ DEAE FF (diethylaminoethyl) or CM FF (carboxymethyl) columns (GE Healthcare Bio-Sciences Inc., Baie d'Urfé, Que.), each 1 mL, connected to a peristaltic pump and mechanical gradient maker, was introduced to purify the proteins further. For TsDHN-1, protein eluted from the first chromatography step was dialysed extensively against 50 mmol·L^{-1} HEPES-NaOH (pH 7.5). The dialysate was loaded at a 1 mL·min^{-1} rate onto the column (DEAE FF) that had been pre-equilibrated with the same buffer, and was eluted with a step gradient of NaCl (40 mmol·L^{-1}, 150 mmol·L^{-1}, and 200 mmol·L^{-1} NaCl) in 20 mL of 50 mmol·L^{-1} HEPES–NaOH (pH 7.5) at 4 °C. The purest fractions of TsDHN-1 were obtained with the 150 mmol·L^{-1} and 200 mmol·L^{-1} NaCl steps, and were pooled. For TsDHN-2, a HiTrap™ CM FF (1 mL) column was used. Protein eluted from the first chromatography step was dialysed extensively against 20 mmol·L^{-1} sodium phosphate buffer (pH 6.6) at 4 °C. The dialysate was loaded onto the column (CM FF) that had been pre-equilibrated with the same buffer at a 1 mL·min^{-1} rate, and was eluted with a step gradient of NaCl (45 mmol·L^{-1}, 75 mmol·L^{-1}, and 175 mmol·L^{-1} NaCl) in 20 mL of 20 mmol·L^{-1} sodium phosphate buffer. The purest fractions of TsDHN-2 were obtained with the 175 mmol·L^{-1} NaCl step, and were pooled.

Purity was assessed by SDS–PAGE with Coomassie Blue R-250 staining. Pure fractions were pooled, extensively dialysed against double-distilled water, and freeze-dried. The protein samples were dissolved in HEPES buffer (20 mmol·L^{-1} HEPES–NaOH, pH 7.5, 100 mmol·L^{-1} NaCl, 1 mmol·L^{-1} ethylenediamine tetraacetic acid (EDTA)) at a concentration of 4 mg·mL^{-1}. Since these proteins lacked tryptophan residues, the extinction coefficients were exceedingly low and we relied only on protein weight and solvent volume to prepare protein solutions with known concentrations. Protein solutions were stored at –20 °C.

Circular dichroism spectroscopy

The protein secondary structure in buffer alone was studied by CD spectroscopy on a JASCO J-815 spectropolarimeter (Japan Scientific, Tokyo) equipped with a recirculating water bath. The scan rates were 50 nm·min^{-1} and the band resolution was 1 nm. The protein concentration in 20 mmol·L^{-1} HEPES–NaOH (pH 7.5), 100 mmol·L^{-1} NaCl was 1.4 mg·mL^{-1} for TsDHN-1 and 1.3 mg·mL^{-1} for TsDHN-2. The CD spectra were collected at 22 °C. Four successive scans were recorded, the sample blank was subtracted, and the scans were averaged. Photobleaching of the samples did not become apparent until 5 or more scans had been performed. The data averaging and smoothing (using the Savitzky-Golay algorithm) operations were accomplished with the OriginPro software package (version 8, OriginLab Corporation, Northampton, Mass.).

Fig. 1. (Note: The full-colour version of the figure is available on the Journal's web site at http://bcb.nrc.ca.) Amino acid sequences and classification of *Thellungiella salsuginea* dehydrins (A) acidic TsDHN-1 and (B) basic TsDHN-2. The colour scheme used is as follows: red, P and acidic residues D, E, N, Q; blue, basic residues H, K, R; green, hydrophobic residues V, L, I, F, W, M, Y; and black, G, S, T, C, A). The Y (consensus sequence (V/T)D(E/Q)YGNP), K (consensus sequence EKKGIMDKIKEKLPG), S (run of 5 or 6 Ser, a phosphorylation sink), and φ (run of polar residues, many Gly) segments are identified. At the amino terminus of each sequence is a Y-like segment that we denote Y′. Dehydrin TsDHN-1 can be classified as K_3S_1, or possibly $Y_1K_4S_1$ if one includes the Y-like segment (denoted Y′) at the amino-terminus, and the lysine-rich cluster (denoted K′) that does not match the consensus as closely. Dehydrin TsDHN-2 can be classified as $Y_2K_3S_1\varphi_9$, or possibly $Y_3K_3S_1\varphi_9$.

(A) Acidic dehydrin TsDHN-1

```
1      MAEEYKNASE EFKNVPEHET TPKISTTEEP SAEVKDRGFF  Y′
41     DFLGKKKEEV KPQETTTPLE SEFEHKAQIS EPPAFVAKHE
81     EEQETKENKP TLVEQLHQKH VEEEENKPSL FDKLHRSSSS  S
121    SSSSSDEEGE DGEKRKKKKE KKKTVEGEDK TEEENKGVMD  K′, K1
161    KIKEKFPHAK KTEDDHAPVV TGVPETEKIG MTEKIKEKLP  K1, K2
201    GHGKKPEDSP VVDTAPVVET ATPITAEHSA EHPAENKGFL  K2, K3
241    EKIKEKLPGH HAKGTEEMEK KEKESDA                K3
```

(B) Basic dehydrin TsDHN-2

```
1      MASYQNRPGA QATDEYGNPM QQLDEYGNPI GGVGATGGGG  Y′, Y, Y, φ
41     AGYGTGGGYG GGATGGEGYG TGALGAGAGA RHHGQEQLHK  φ, φ, φ
81     EGGGGLGGML HRSGSGSSSS SEDDGQGGRR KKGITQKIKE  φ, S, K1
121    KLPGQHDQSG QSQGMGMGTT TGYDAGGYGG QHHEKKGITD  K1, φ, K2
161    KIKEKLPGQD QSGQSQGMGM GATTGYDAGG YGGERHEKKG  K2, φ, φ, K3
201    MMDKIKDKLP GGGGR                             K3, φ
```

Lipids and vesicle preparation for transmission-FTIR spectroscopy

Various lipid stocks in chloroform or in chloroform : H_2O : methanol (1:2:1 by volume) mixtures were prepared at the desired mass ratio. The solvent was then evaporated under a mild flow of nitrogen gas and subsequently kept under vacuum overnight for complete removal of the chloroform remnants. Lipid mixtures were rehydrated in buffer (20 mmol·L^{-1} HEPES–NaOH, pH 7.5, 100 mmol·L^{-1} NaCl) at room temperature overnight with vigorous shaking and three freeze–thaw cycles.

Large unilamellar vesicles (LUVs) were formed by extruding lipid mixtures (61 times at 45 °C) through a polycarbonate membrane with a 100 nm pore size. The lipid compositions were chosen to mimic the plant plasma (PC:PS:PI, 33:47:20 by mass ratio), mitochondrial (PC:PS:PE:Chol, 27:25:29:20 by mass ratio), or chloroplast (MGDG:DGDG:SQDG:PC:PG:PI, 51:26:7:3:9:1 by mass ratio) membranes (Harwood 1980). The sizes of vesicles were approximately 100 nm, as measured by dynamic light scattering (DLS) Zetasizer Nano-S model ZEN1600 (633 nm "red" laser; Malvern Instruments). The desired amount of protein (in 20 mmol·L^{-1} HEPES–NaOH, pH 7.5, 100 mmol·L^{-1} NaCl) was added to the LUVs at a lipid-to-protein ratio of either 1:1 or 3:1 by mass. The protein–LUV complexes were used within 1 h of preparation for FTIR measurements. The lipid-to-protein ratio was chosen to assure a significant signal-to-noise ratio.

Transmission-Fourier transform infrared (FTIR) spectroscopy

The transmission-FTIR spectra were recorded between 950 and 1800 cm^{-1} using a Bruker Optics IFS 66v/S FTIR spectrometer. The temperature was controlled with an Isotemp 3006 temperature controller (Fisher Scientific) with 0.1 degree resolution. The protein–lipid vesicle complexes were dried onto a CaF_2 window with a mild vacuum for ~40 min to give a thin homogeneous film. Before use, the CaF_2 window was cleaned with methanol, followed by MilliQ H_2O. To maintain the physiological condition of the proteins, the complex was spread into a thin film prepared with 2 μL of 20 mmol·L^{-1} HEPES–NaOH, pH 7.5, 100 mmol·L^{-1} NaCl, 1 mmol·L^{-1} ethelynediamine tetraacetic acid (EDTA). Briefly, 2 μL of the buffer was dried on a clean CaF_2 window for 10 min under vacuum. Then, the dried buffer was spread into a thin film covering a circular area on the window (diameter 1 cm) with 2 μL MilliQ H_2O using a pipette tip. Next, the protein–lipid vesicle complexes were deposited and dried onto this CaF_2 window with a mild vacuum for ~40 min to give a thin homogeneous film. Significantly better signal-to-noise ratios were achieved with a second deposition of film on the window.

The spectral region most sensitive to peptide backbone conformation is the amide I band region, which is located between 1700 and 1600 cm^{-1}. However, water has a strong IR absorbance peak at ~1645 cm^{-1}, due to H-O-H bending, which overlaps the amide I band. Thus, analysis of protein secondary structure is difficult in a pure H_2O environment. Here, to be able to probe protein secondary structure without the interference of water absorbance, all measurements were performed in a D_2O environment. To deuterate the protein completely, heavy water (an amount of 4 μL D_2O) was deposited onto the protein-lipid film. This amount of D_2O was optimized for maximum hydrogen–deuterium (H–D) exchange, which occurred within 5 min. Any additional

Fig. 2. Disorder, charge, and hydrophobicity analyses of (A, C, E, G) TsDHN-1 and (B, D, F, H) TsDHN-2. (A and B) Degree of disorder as predicted by the IUPred server (http://iupred.enzim.hu/). (C and D) Net charge calculated over an 11-residue window. (E and F) Average hydrophobicity calculated over an 11-residue window. (G and H) Hydrophobic moment calculated over an 11-residue window. The grey bars represent the regions of the K segments, which all display strong hydrophobic moments.

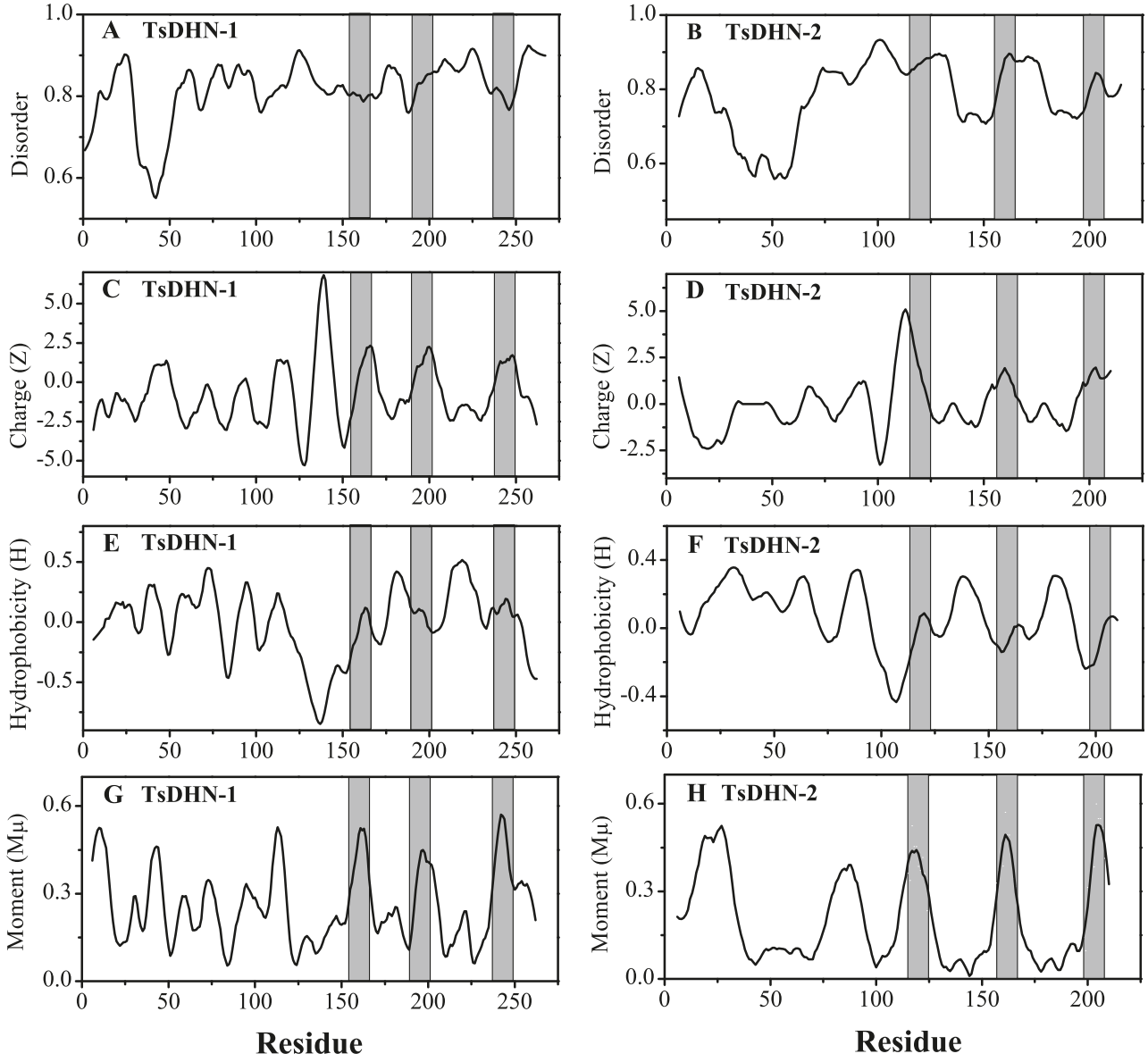

amount of D_2O would not cause any further change in the amide I and II regions.

The thickness of the film in the FTIR sample holder was controlled with a 6 μm spacer (Harrick Scientific Corporation, Ossining, N.Y.). For samples with 1:1 lipid-to-protein ratios, experiments were conducted at temperatures ranging from 22 to 2 °C, with 5 °C intervals. For samples with 3:1 lipid-to-protein ratios, these temperatures were 22 °C, 12 °C, and 7 °C. For each spectrum, 1000 interferograms were collected and Fourier-transformed to give a resolution of 4 cm^{-1}. The amount of protein required for each experiment was ~0.5 mg.

Transmission-FTIR data analysis

The overlapping bands in transmission-FTIR spectra were resolved by Fourier self-deconvolution (FSD) using OMNIC software (Thermo Fisher Scientific, Waltham, Mass.). The bandwidth at half-height was set to 15 cm^{-1}, and the enhancement value was set to 1.8. The number and the location of peaks of the secondary structure components were verified by the second derivative method using the PeakFit program (version 4.12, Seasolve Software Inc., San Jose, Calif.). The conditions were chosen such that the increase in noise and appearance of side chain lobe were minimal while maximum band narrowing was achieved.

The observed amide I bands of proteins thus consisted of overlapping secondary structure component bands. The spectra of the TsDHN-1 or TsDHN-2 proteins reconstituted in LUVs were deconvoluted using a mixed Gaussian and Lorentzian band shape. Auto-fits of the self-deconvoluted

Fig. 3. Sodium dodecyl sulphate polyacrylamide gel electrophoresis of (A) TsDHN-1 (major band at roughly 48 kDa, predicted M_r 30140.3 Da), and (B) TsDHN-2 (major band at roughly 24 kDa, predicted M_r 21435.1 Da). The molecular masses of markers are indicated in kDa.

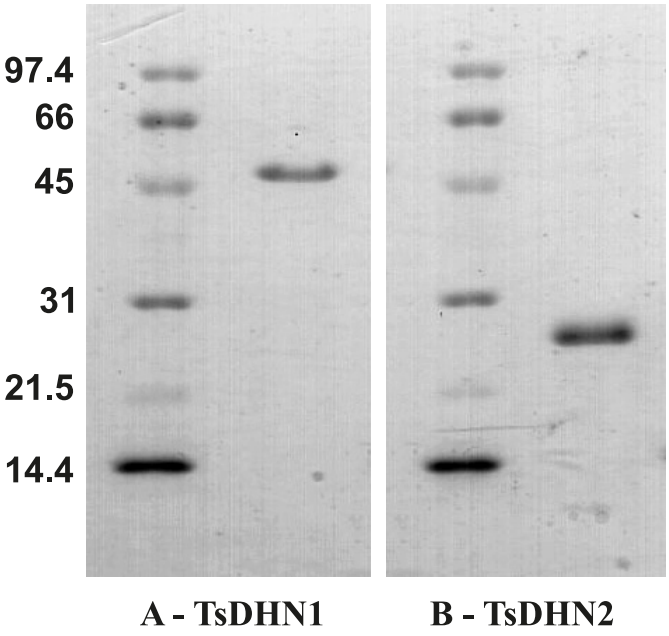

spectra of the original spectra were performed until the coefficient of determination (r^2) was larger than 0.99. The integrated areas derived from the curve-fitting analyses were used in calculating the various conformational states assigned to individual bands.

The wave numbers of these component bands were subsequently used in PeakFit as input parameters for curve-fitting analysis of the amide I original spectrum. The parameters were left free to adjust iteratively, with the only restriction on the peak wavenumbers being to vary within a range of ±2 cm^{-1} (Arrondo et al. 1993). The amide I region (~1600–1700 cm^{-1}) arises due to the peptide backbone C=O stretching, and some in-plane N–H bending in a pure H_2O environment. Since all the FTIR measurements were done in a saturated D_2O environment, the band located between 1700 and 1600 cm^{-1} can be considered to be due to only C=O stretching.

Results and discussion

Primary structure analysis of *Thellungiella salsunigea* dehydrins

Thellungiella salsunigea is a crucifer with an exceptional capacity to withstand environments associated with low water availability. The Yukon ecotype thrives in the Canadian sub-Arctic, where it grows on saline-rich soils and experiences periods of both cold and drought (Griffith et al. 2007). To begin to understand the molecular basis of *Thellungiella*'s unusual abiotic stress tolerance, Wong and colleagues created expressed-sequence tag (EST) collections of cold, salinity, or drought-induced *Thellungiella* transcripts, and found that dehydrin sequences were particularly abundant in all 3 libraries (Wong et al. 2005, 2006).

Fig. 4. CD spectroscopy of (A) TsDHN-1 and (B) TsDHN-2 in aqueous buffer at 22 °C. The spectra are representative of a primarily random-coil conformation of each protein under these conditions.

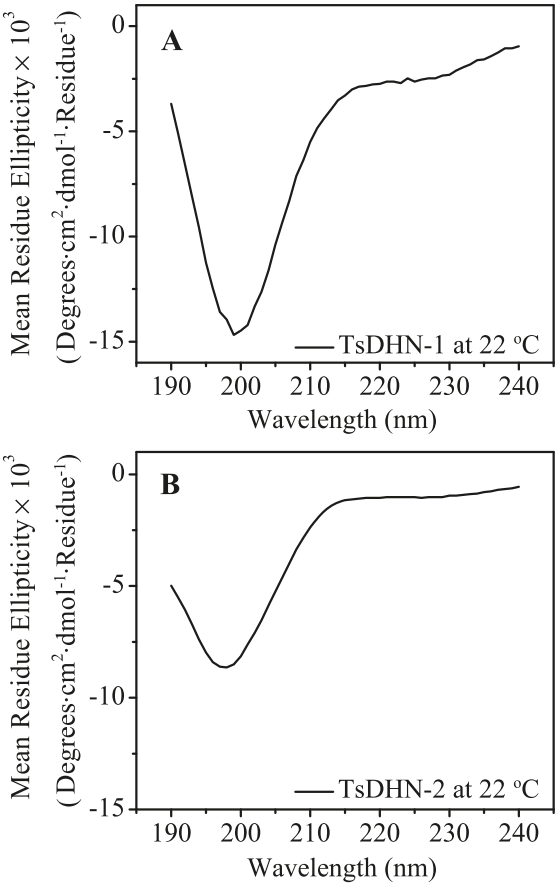

We selected two dehydrins for detailed characterization. These proteins were designated as TsDHN-1 and TsDHN-2. We first performed several simple bioinformatic analyses of the amino acid sequences of these *Thellunigiella* dehydrins using online tools. First of all, visual inspection of the amino acid sequences shows that both dehydrins (Fig. 1) are comparable with known dehydrins in terms of their Y-K-S classification (listed in Battaglia et al. (2008)). The primary sequence analysis suite at http://www.expasy.ch yields that TsDHN-1 is acidic (267 residues, M_r 30140.3 Da, calculated pI 5.25, net charge –19 at neutral pH) and that TsDHN-2 is slightly basic (215 residues, M_r 21435.1 Da, calculated pI 7.91, net charge +1 at neutral pH). These differences in acidity may impart on them different physiological roles. In the TsDHN-1 dehydrin, there is a lysine-rich cluster (denoted K′ in Fig. 1) that does not match the consensus, but that will nevertheless interact with a phospholipid membrane, as could be predicted by analogy with the lysine-rich MARCKS (myristoylated alanine-rich C-kinase substrate) motif (Arbuzova et al. 1998). Moreover, several internal repeats are predicted by the RADAR (Rapid Automatic Detection and Alignment of Repeats) program in this primary sequence analysis suite.

Several further analyses of the TsDHN-1/2 sequences are presented in Fig. 2. First of all, both proteins are predicted

Fig. 5. Changes in CD spectra for (A, C, E) TsDHN-1 and (B, D, F) TsDHN-2 in association with large unilamellar vesicles, all at a lipid-to-protein ratio of 1:1. The lipid compositions mimic the plant plasma (A and B), chloroplast (C and D) or mitochondrial (E and F) membranes. Plots represent the difference of spectra in the presence and absence of lipids.

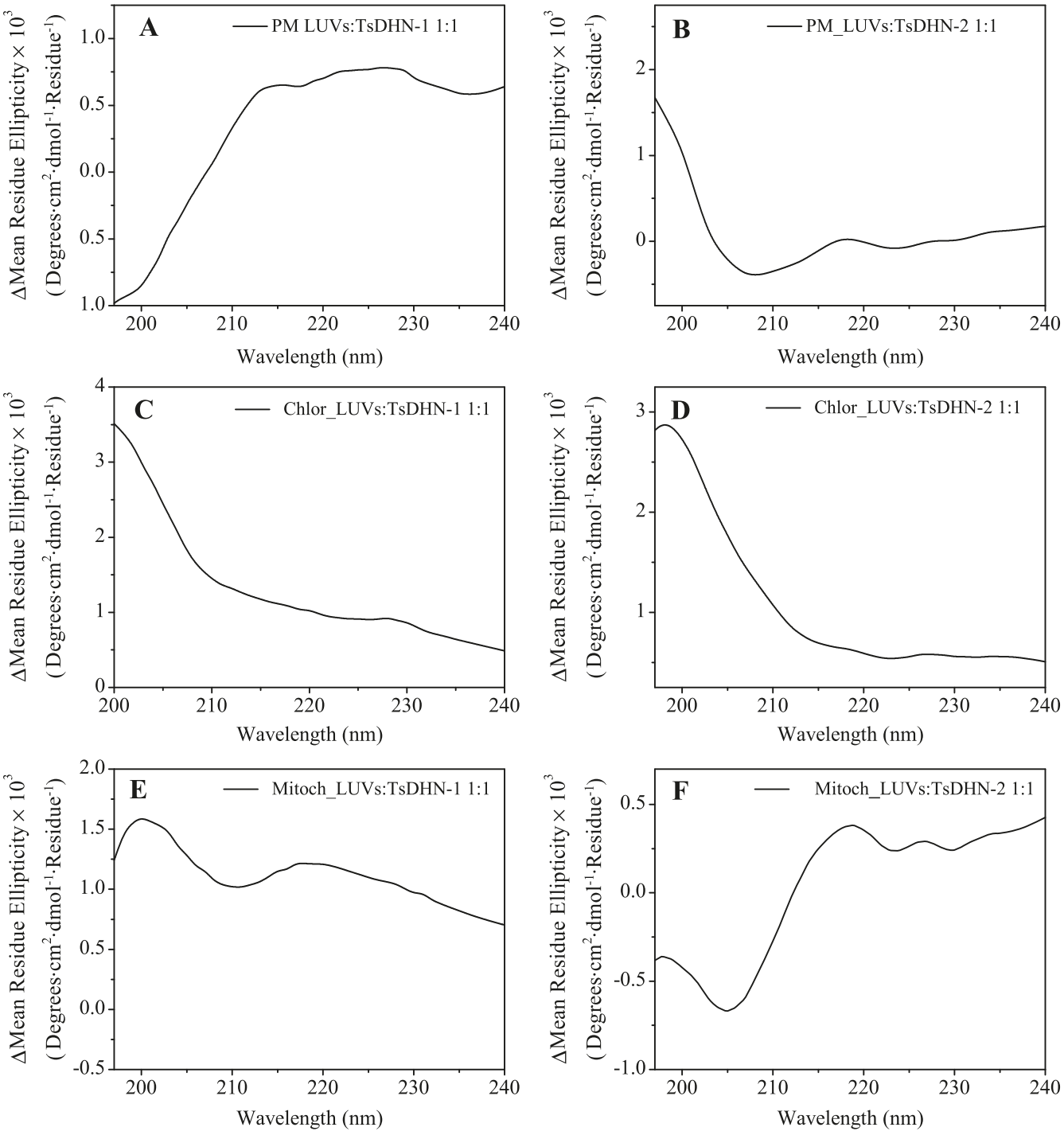

to be largely intrinsically disordered (unstructured) using the IUPred program (Figs. 2A and 2B) (Dosztányi et al. 2005). Using our own program, and a moving window of 11 residues (three turns of an α-helix), we calculated several other physicochemical properties as a function of position. Both *Thellungiella* dehydrins have regions that vary in net charge (Figs. 2C and 2D), and average hydrophobicity (Figs. 2E and 2F), for which we used the hydrophobic scale of Fauchère and Pliska (1983). Using this hydrophobicity scale, we calculated the helical hydrophobic moment as a function of position (Figs. 2G and 2H). Several segments are shown to have high hydrophobic moments, suggesting that they may form amphipathic α-helices that would be advantageous for membrane association.

Purification of recombinant *Thellungiella salsunigea* dehydrins

The cDNAs encoding TsDHN-1 and TsDHN-2 were cloned into the intein-containing vector pTYB2 to express each protein as a fusion with a chitin-binding domain. The recombinant proteins were efficiently recovered from the supernatant of extracts of transformed cells by affinity chromatography. The chitin-binding tags were auto-catalytically removed from each dehydrin by the addition of dithiothreitol during the elution step of the purification. We optimized the purification of recombinant TsDHN-1 and TsDHN-2 using ion exchange chromatography to recover protein with a high degree of purity (Fig. 3). The abnormal migration of TsDHN-1 is due to its high net charge and is characteristic of intrinsically disordered proteins (Receveur-Bréchot et al. 2006). The yield of each protein was typically 2 mg from 1 L of culture in shaker flasks, which scaled up in the fermentor to 100 mg from 1 L of culture.

Protein secondary structure analysis by CD and transmission-FTIR spectroscopy

We initially performed CD spectroscopy of TsDHN-1 and TsDHN-2 in aqueous solution, with the results showing that these proteins are relatively unstructured under such conditions (Fig. 4), consistent with other intrinsically disordered proteins such as myelin basic protein (Polverini et al. 1999; Harauz et al. 2004). Upon mixing with LUVs at either a 1:1 or 3:1 lipid-to-protein ratio, the CD spectra of both proteins demonstrated changes consistent with ordered secondary structure formation (Fig. 5). However, it was not possible to quantify the degree of change because of light scattering even at relatively low lipid-to-protein ratios, and we next turned to transmission-FTIR spectroscopy of semi-solid samples with which scattering was not a limiting factor.

The secondary structure compositions of TsDHN-1 and TsDHN-2 were investigated by transmission-FTIR spectroscopy of these proteins alone and when associated with LUVs of three different lipid compositions, mimicking the plant plasma (PC:PS:PI, 33:47:20, mass ratio), mitochondrial (PC:PS:PE:Chol, 27:25:29:20, mass ratio), and chloroplast (MGDG:DGDG:SQDG:PC:PG:PI, 51:26:7:3:9:1, mass ratio) membranes (Harwood 1980). The amide I band in the transmission-FTIR spectra, located between 1700 and 1600 cm^{-1}, is often used to estimate the secondary structure composition of proteins (Jung 2000). The different secondary structure components are usually hidden by the broadness of the bands in the raw transmission-FTIR spectra, and curve-fitting and band-narrowing methods are required to decompose them into different components (Byler and Susi 1986; Krimm and Bandekar 1986; Surewicz and Mantsch 1988; Bandekar 1992; Surewicz et al. 1993; Goormaghtigh et al. 2009). Nevertheless, there is considerable variability in published predictions (Goormaghtigh et al. 2009; Laird et al. 2009).

To illustrate this process, we show an unprocessed transmission-FTIR spectrum of TsDHN-1 associated with chloroplast-LUVs at a lipid-to-protein ratio of 1:1 in D_2O in Fig. 6A. In Fig. 6B, we show the secondary structure analysis obtained from this spectrum using PeakFit Software. Because partial overlap of the amide I bands was observed, as well as overlap of the bands (1585 cm^{-1}) associated with the side chains, both sets of bands were fitted with multiple Gaussian and Lorentzian peaks, but only the peaks under the amide I band were used in the calculation of protein secondary structure. All infrared spectra were normalized by rescaling them, such that the area between the baseline (which was linear) and the spectra within the region of 1775 and 1485 cm^{-1} was unity. In this study, all spectra were processed consistently in this manner. Detailed predictions of the proportions of different types of secondary structures (α-helix, β-strand, anti-parallel β-sheet, and random coil) are given in the Appendix (Tables A1–A8). It should be cautioned that the calculations of overall secondary structure composition from such spectra may vary depending on the type of peak identification and fitting performed (Barth 2007; Goormaghtigh et al. 2009; Laird et al. 2009). Moreover, the absorbance maximum of the band associated with the random-coil conformation shifts from 1655 to 1645 cm^{-1} upon hydrogen–deuterium (H–D) exchange. The strength and length of hydrogen bonds are affected by H–D

Fig. 6. (A) Fourier self-deconvolution of an unprocessed transmission-FTIR spectrum of TsDHN-1, associated with chloroplast LUVs at a lipid-to-protein ratio of 1:1 in D_2O at 22 °C, using OMNIC software with a bandwidth at a half-height of 15 cm^{-1} and an enhancement value of 1.8. (B) Analysis of the transmission-FTIR spectrum (derived from panel A) for secondary structure determination by PEAKFIT software; the baseline-corrected spectra of the TsDHN-1 or TsDHN-2 proteins reconstituted in LUVs of differing lipid compositions were deconvoluted using a mixed Gaussian and Lorentzian band shape. Auto-fits of the self-deconvoluted spectra of the original spectra were performed until the coefficient of determination (r^2) was larger than 0.99, and the bandwidths of the secondary structure components were ~22 cm^{-1}.

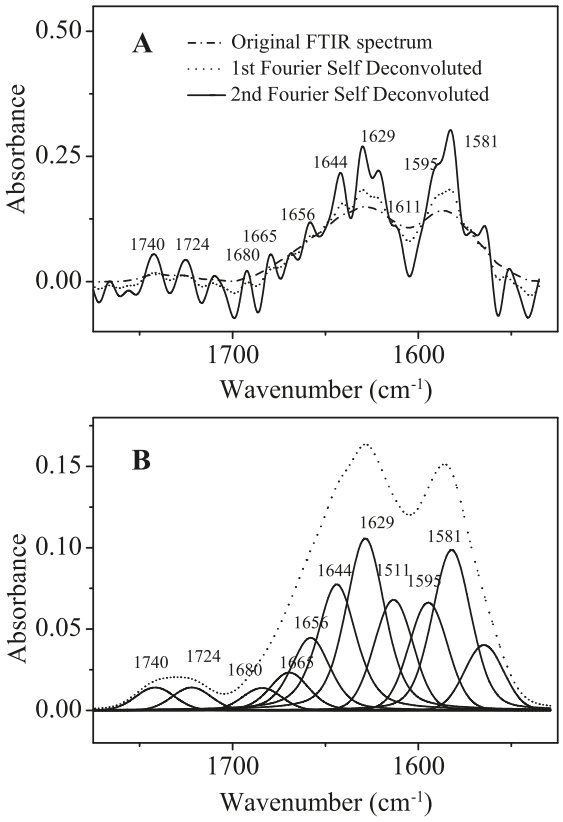

Fig. 7. Effect of temperature on proportion of ordered secondary structure (α-helix, β-strand, or β-turn) determined using transmission-FTIR spectroscopy of (A and C) TsDHN-1 and (B and D) TsDHN-2 in association with large unilamellar vesicles, all at lipid-to-protein ratio of 1:1 in D_2O. The lipid compositions mimic either (A and B) the plant plasma membrane (PC:PE:PI at 33:47:20) or (C and D) the chloroplast membrane (MGDG:DGDG:SQDG:PC:PG:PI, 51:26:7:3:9:1). Error bars represent the standard deviation of duplicate measurements. (This experiment was not performed with vesicles mimicking mitochondrial membranes.)

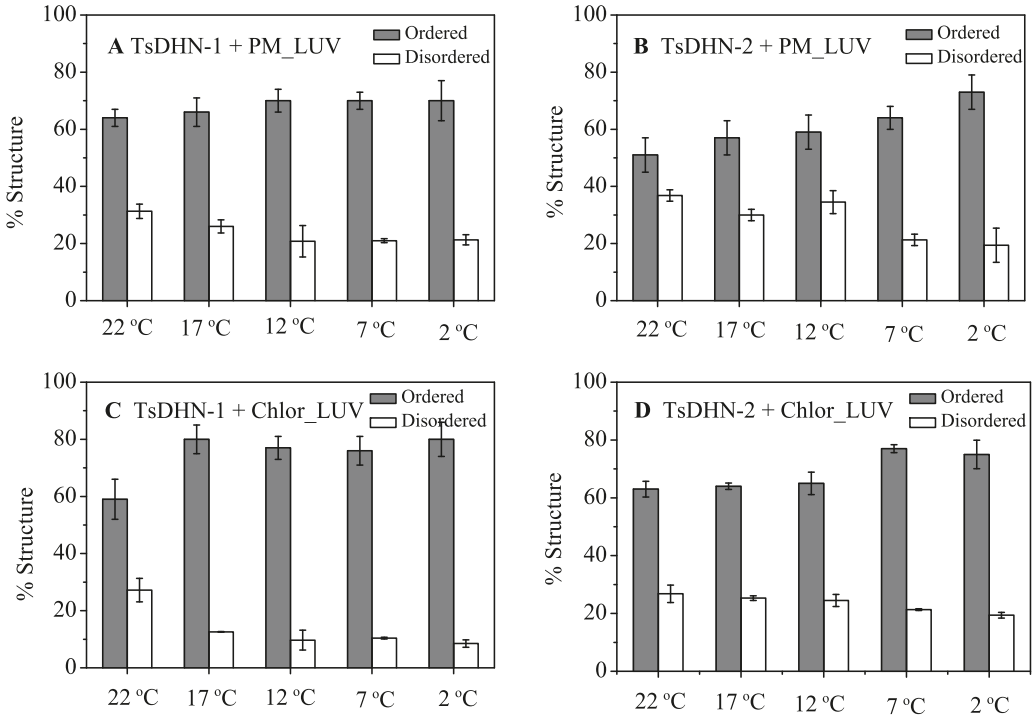

exchange, which may slightly affect the secondary structure. For these reasons, then, we restrict ourselves here simply to reporting on trends in change in secondary structure composition in each set of experiments, and disorder-to-order transitions, which we can do confidently given that all data were analyzed consistently.

Effect of temperature on the secondary structure composition of dehydrins

The effects of temperature on the degree of ordered secondary structure of TsDHN-1 and TsDHN-2, associated with LUVs with lipid compositions mimicking those of plant plasma and chloroplast membranes, and at a 1:1 lipid-to-protein ratio, are shown in Fig. 7. The detailed predictions of different types of secondary structures are given in Appendix A (Tables A1–A4). The transmission-FTIR spectra of both TsDHN-1 and TsDHN-2 show a peak at 1643–1645 cm^{-1}, the signature of the random-coil conformation (Byler and Susi 1986; Krimm and Bandekar 1986; Surewicz and Mantsch 1988; Bandekar 1992; Surewicz et al. 1993). Moreover, parallel β-strands (peaks at 1620 and 1632 cm^{-1}), anti-parallel β-strands (peaks at 1676–1681 cm^{-1}), and turns (peaks at 1690–1693 cm^{-1}) are indicated. The peaks at 1664–1665 cm^{-1} can be assigned to either turns (Byler and Susi 1986) or to a 3_{10} helix (Surewicz et al. 1993). The latter conformation is relatively rare in proteins, however. Here, we combine predictions of parallel and anti-parallel β-strands as recently recommended (Barth 2007). We consider ordered secondary structure to be the sum of everything other than the unstructured random-coil conformation.

The PeakFit analysis of the transmission-FTIR spectrum of TsDHN-1 associated with plasma membrane (PM) LUVs at room temperature, and at a 1:1 lipid-to-protein ratio, suggests that 30% of the total structure is random coil (Fig. 7A; Table A1). The β-strands and α-helical structures are estimated to be 31% and 18%, respectively. With decreasing temperature, an increase in proportion of ordered secondary structures is observed, e.g., at 2 °C the proportion of random coil in TsDHN-1 is estimated to be 21%, compared with 30% at room temperature. The secondary structure estimation for TsDHN-2 reconstituted with PM-LUVs at room temperature included 38% random coil, 24% β-sheet, and 28% α-helical structures (Fig. 7B; Table A2), suggesting that TsDHN-2 is less ordered than TsDHN-1 at room temperature in this environment.

In contrast with PM LUVs, when associated with chloroplast LUVs, the amounts of random coil estimated in TsDHN-1 (27%) or TsDHN-2 (26%) decrease at room temperature (Fig. 7C; Tables A3 and A4, respectively). At low temperature, TsDHN-1 becomes significantly more ordered (by 19%, Fig. 7C). The ordered structure content of TsDHN-2 also increases at low temperature, but not as dramatically (only 8%, Fig. 7D).

The solution CD and semisolid-state transmission FTIR studies were done at different protein concentrations out of necessity. We additionally performed a control transmission FTIR experiment in which we analyzed protein alone without LUVs (Table A5). The results indicated that both proteins had primarily a random-coil composition, slightly reduced at a lower temperature.

Fig. 8. Effect of temperature on secondary structure composition (α-helix, β-strand, β-turn, or random coil), determined using transmission-FTIR spectroscopy of (A, C, E) TsDHN-1 and (B, D, F) TsDHN-2 in association with large unilamellar vesicles, all at a lipid-to-protein ratio of 3:1. The lipid compositions mimic the (A and B) plant plasma, (C and D) chloroplast, or (E and F) mitochondrial membranes. Error bars represent the standard deviation of duplicate measurements.

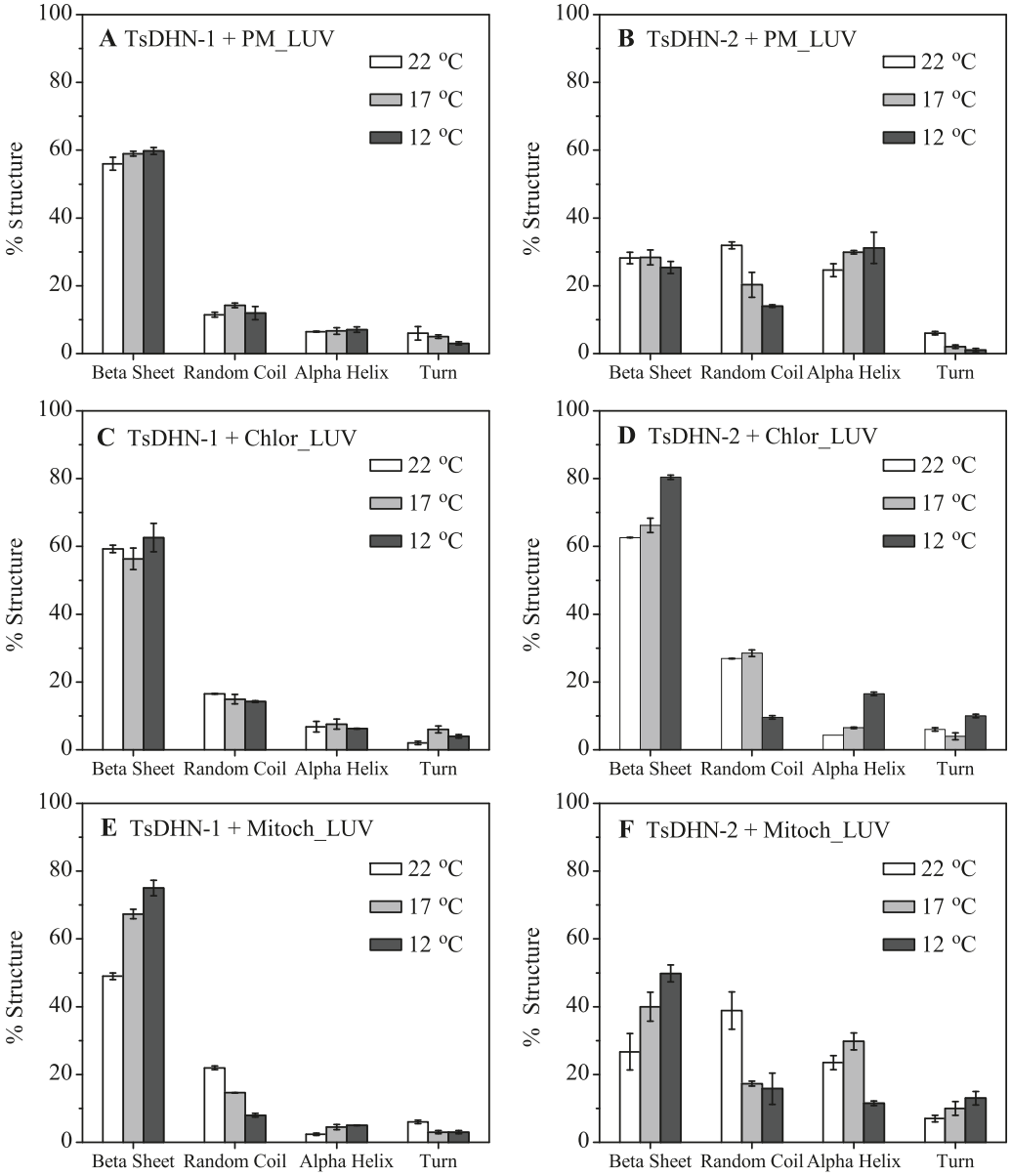

Collectively, these results show that both dehydrins gain ordered secondary structure upon association with lipid bilayers mimicking plant membranes, and that these induced structures appear to be stabilized further at cold temperatures. These former results are generally consistent with studies on other dehydrins, e.g., it has been shown that DHN-1 from *Zea mays* has a preferential binding to vesicles containing acidic phospholipids such as phosphatidylinositol or phosphatidic acid (Koag et al. 2003). (These authors also indicated a preferential binding to vesicles of greater curvature, particularly 20–60 nm vs. 100 nm diameter vesicles, a phenomenon we did not investigate here.) Our latter results on *Thellungiella* TsDHN-1 and TsDHN-2 are also consistent with other observations of cold-stability of intrinsically disordered proteins (Tantos et al. 2009).

Effects of lipid composition and lipid-to-protein ratio on secondary structure composition

To further investigate the effects of types of lipids on the secondary structure compositions of the dehydrins, we reduced the amount of protein in the reconstituted systems. Both TsDHN-1 and TsDHN-2 have higher proportions of β-sheet structure at a high lipid-to-protein ratio of 3:1 with mitochondrial LUVs than with plasma membrane or chloroplast LUVs (Fig. 8; Tables A6–A8). TsDHN-1 has more β-sheet structure (above 50%) with all three lipid compositions studied at a 3:1 lipid-to-protein ratio (Figs. 8A, 8C, and 8E; Tables A6–A8), compared with ~35% β-sheet at a 1:1 lipid-to-protein ratio (Tables A1 and A3). The transformation of α-helical structure to β-sheet structure with increasing LUV concentration has been observed in previous studies on other

Fig. 9. Effect of temperature on proportion of ordered secondary structure (α-helix, β-strand, or β-turn), determined using transmission-FTIR spectroscopy of (A, C, E) TsDHN-1 and (B, D, F) TsDHN-2 in association with large unilamellar vesicles, all at a lipid-to-protein ratio of 3:1. The lipid compositions mimic the (A and B) plant plasma, (C and D) chloroplast, or (E and F) mitochondrial membranes. Error bars represent the standard deviation of duplicate measurements.

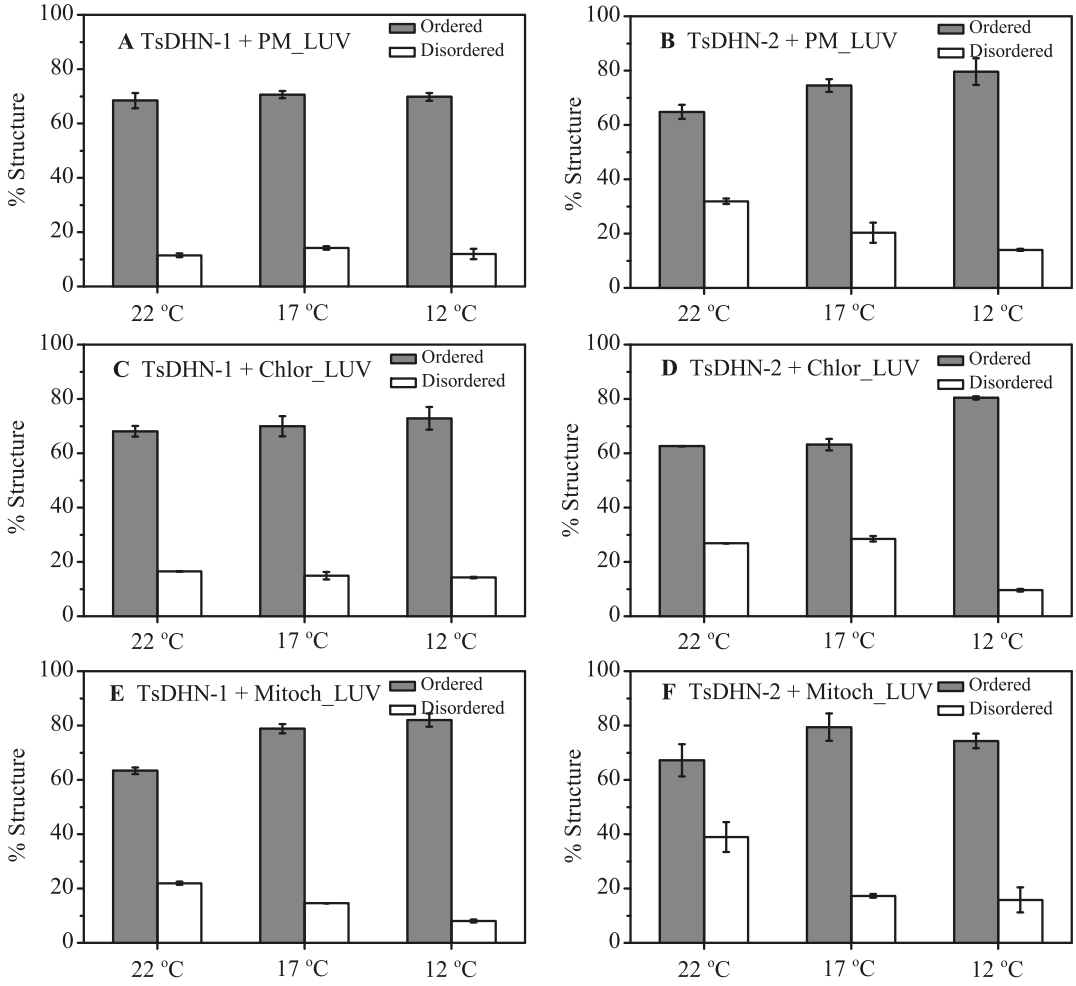

proteins (Terzi et al. 1997; Wieprecht et al. 1999; Vié et al. 2000). The reason for the transformation of the random-coil structure or α-helical conformations to β-sheet at large lipid-to-protein ratios is possibly due to the increased penetration of the protein into the membrane. The disorder-to-order transition with decreasing temperature (when the lipid-to-protein ratio is 3:1) is greatest with TsDHN-1 and mitochondrial membrane-mimicking LUVs (Fig. 9E), and with TsDHN-2 with both plasma membrane and chloroplast membrane-mimicking LUVs (Figs. 9B and 9D, respectively). In these experiments done at the higher lipid-to-protein ratios, we suggest that protein–protein interactions would be decreased. However, we cannot presently unravel the contribution of any such interactions to the induced secondary structure stabilization, and cannot discount the possibility of increased protein–protein interactions in vivo, a situation that may arise at high levels of dehydrin expression.

Conclusions

We have investigated the interactions of *Thellungiella salsuginea* dehydrins TsDHN-1 and TsDHN-2 with membranes of diverse lipid composition in vitro to gain further insight into their physiological roles. Using spectroscopic methods, we have shown that both proteins associate with membranes mimicking those found in plants, and thereby gain ordered secondary structure. These observations are consistent with other dehydrins from other plants that have been investigated (Soulages et al. 2002, 2003; Koag et al. 2003, 2009). The basic dehydrin TsDHN-2 most likely interacts electrostatically with the phospholipid membranes, and both dehydrins most likely interact peripherally via their K-segments. Decreasing temperature appears to stabilize both proteins, consistent with studies on other intrinsically disordered proteins, including dehydrins (Tantos et al. 2009). These strong membrane interactions of both dehydrins, with concomitant induced folding (ordered secondary structure formation), support the hypothesis that they associate with and protect plant plasma and organellar membranes under conditions of extreme cold (Beck et al. 2007; Zhang et al. 2010). It would be anticipated that other dehydrins would behave similarly, and future in situ studies would shed further light on their roles.

Acknowledgements

This work was supported by the Advanced Foods and Materials Network (AFMNet) of the National Centres of Excellence (Natural Sciences and Engineering Research Council of Canada). J.R.D. acknowledges support from the Canada Research Chair Program. The authors are grateful to Mr. Kyrylo Bessonov for compiling Fig. 2, to Dr. Frances Sharom (Guelph) for the use of her Zetasizer DLS instrument, to Dr. Leonid Brown (Guelph) for the use of his transmission-FTIR spectrometer, and to Dr. Brown and Dr. Mylene Miranda (Guelph) for assistance with the transmission-FTIR spectroscopic experiments and analyses of results.

References

Allagulova, ChR., Gimalov, F.R., Shakirova, F.M., and Vakhitov, V.A. 2003. The plant dehydrins: structure and putative functions. Biochemistry (Mosc.), **68**(9): 945–951. doi:10.1023/A:1026077825584. PMID:14606934.

Alsheikh, M.K., Heyen, B.J., and Randall, S.K. 2003. Ion binding properties of the dehydrin ERD14 are dependent upon phosphorylation. J. Biol. Chem. **278**(42): 40882–40889. doi:10.1074/jbc.M307151200. PMID:12917402.

Amtmann, A. 2009. Learning from evolution: *Thellungiella* generates new knowledge on essential and critical components of abiotic stress tolerance in plants. Mol Plant, **2**(1): 3–12. doi:10.1093/mp/ssn094. PMID:19529830.

Arbuzova, A., Murray, D., and McLaughlin, S. 1998. MARCKS, membranes, and calmodulin: kinetics of their interaction. Biochim. Biophys. Acta, **1376**(3): 369–379. PMID:9804991.

Arrondo, J.L., Muga, A., Castresana, J., and Goñi, F.M. 1993. Quantitative studies of the structure of proteins in solution by Fourier-transform infrared spectroscopy. Prog. Biophys. Mol. Biol. **59**(1): 23–56. doi:10.1016/0079-6107(93)90006-6. PMID:8419985.

Bandekar, J. 1992. Amide modes and protein conformation. Biochim. Biophys. Acta, **1120**(2): 123–143. PMID:1373323.

Barth, A. 2007. Infrared spectroscopy of proteins. Biochim. Biophys. Acta, **1767**(9): 1073–1101. doi:10.1016/j.bbabio.2007.06.004. PMID:17692815.

Battaglia, M., Solórzano, R.M., Hernández, M., Cuéllar-Ortiz, S., García-Gómez, B., Márquez, J., and Covarrubias, A.A. 2007. Proline-rich cell wall proteins accumulate in growing regions and phloem tissue in response to water deficit in common bean seedlings. Planta, **225**(5): 1121–1133. doi:10.1007/s00425-006-0423-9. PMID:17109151.

Battaglia, M., Olvera-Carrillo, Y., Garciarrubio, A., Campos, F., and Covarrubias, A.A. 2008. The enigmatic LEA proteins and other hydrophilins. Plant Physiol. **148**(1): 6–24. doi:10.1104/pp.108.120725. PMID:18772351.

Beck, E.H., Fettig, S., Knake, C., Hartig, K., and Bhattarai, T. 2007. Specific and unspecific responses of plants to cold and drought stress. J. Biosci. **32**(3): 501–510. doi:10.1007/s12038-007-0049-5. PMID:17536169.

Bravo, L.A., Gallardo, J., Navarrete, A., Olave, N., Martinez, J., Alberdi, M., et al. 2003. Cryoprotective activity of a cold-induced dehydrin purified from barley. Physiol. Plant. **118**(2): 262–269 . ISI:000182797600012 doi:10.1034/j.1399-3054.2003.00060.x.

Byler, D.M., and Susi, H. 1986. Examination of the secondary structure of proteins by deconvolved FTIR spectra. Biopolymers, **25**(3): 469–487. doi:10.1002/bip.360250307. PMID:3697478.

Campbell, S.A., and Close, T.J. 1997. Dehydrins: Genes, proteins, and associations with phenotypic traits. New Phytol. **137**(1): 61–74. doi:10.1046/j.1469-8137.1997.00831.x.

Caramelo, J.J., and Iusem, N.D. 2009. When cells lose water: Lessons from biophysics and molecular biology. Prog. Biophys. Mol. Biol. **99**(1): 1–6. doi:10.1016/j.pbiomolbio.2008.10.001. PMID:18977383.

Carjuzaa, P., Castellión, M., Distéfano, A.J., del Vas, M., and Maldonado, S. 2008. Detection and subcellular localization of dehydrin-like proteins in quinoa (*Chenopodium quinoa* Willd.) embryos. Protoplasma, **233**(1–2): 149–156. doi:10.1007/s00709-008-0300-4. PMID:18648732.

Ceccardi, T.L., Meyer, N.C., and Close, T.J. 1994. Purification of a maize dehydrin. Protein Expr. Purif. **5**(3): 266–269. doi:10.1006/prep.1994.1040. PMID:7950370.

Chong, S., Mersha, F.B., Comb, D.G., Scott, M.E., Landry, D., Vence, L.M., et al. 1997. Single-column purification of free recombinant proteins using a self-cleavable affinity tag derived from a protein splicing element. Gene, **192**(2): 271–281. doi:10.1016/S0378-1119(97)00105-4. PMID:9224900.

Close, T.J. 1997. Dehydrins: A commonality in the response of plants to dehydration and low temperature. Physiol. Plant. **100**(2): 291–296. doi:10.1111/j.1399-3054.1997.tb04785.x.

Danyluk, J., Perron, A., Houde, M., Limin, A., Fowler, B., Benhamou, N., and Sarhan, F. 1998. Accumulation of an acidic dehydrin in the vicinity of the plasma membrane during cold acclimation of wheat. Plant Cell, **10**(4): 623–638. doi:10.1105/tpc.10.4.623. PMID:9548987.

Dosztányi, Z., Csizmok, V., Tompa, P., and Simon, I. 2005. IUPred: web server for the prediction of intrinsically unstructured regions of proteins based on estimated energy content. Bioinformatics, **21**(16): 3433–3434. doi:10.1093/bioinformatics/bti541. PMID:15955779.

Eom, J.W., Baker, W.R., Kintanar, A., and Wurtele, E.S. 1996. The embryo-specific EMB-1 protein of *Daucus carota* is flexible and unstructured in solution. Plant Sci. **115**(1): 17–24. ISI:A1996UB82800003 doi:10.1016/0168-9452(96)04332-4.

Fauchère, J.L., and Pliska, V. 1983. Hydrophobic parameters P of amino acid side chains from the partitioning of N-acetyl-amino acid amides. Eur. J. Med. Chem. **18**(3): 369–375.

Garay-Arroyo, A., Colmenero-Flores, J.M., Garciarrubio, A., and Covarrubias, A.A. 2000. Highly hydrophilic proteins in prokaryotes and eukaryotes are common during conditions of water deficit. J. Biol. Chem. **275**(8): 5668–5674. doi:10.1074/jbc.275.8.5668. PMID:10681550.

Goldgur, Y., Rom, S., Ghirlando, R., Shkolnik, D., Shadrin, N., Konrad, Z., and Bar-Zvi, D. 2007. Desiccation and zinc binding induce transition of tomato abscisic acid stress ripening 1, a water stress- and salt stress-regulated plant-specific protein, from unfolded to folded state. Plant Physiol. **143**(2): 617–628. doi:10.1104/pp.106.092965. PMID:17189335.

Goormaghtigh, E., Gasper, R., Benard, A., Goldsztein, A., and Raussens, V. 2009. Protein secondary structure content in solution, films and tissues: redundancy and complementarity of the information content in circular dichroism, transmission and ATR FTIR spectra. Biochim. Biophys. Acta, **1794**(9): 1332–1343. doi:10.1016/j.bbapap.2009.06.007. PMID:19540367.

Griffith, M., Timonin, M., Wong, A.C., Gray, G.R., Akhter, S.R., Saldanha, M., et al. 2007. *Thellungiella*: an *Arabidopsis*-related model plant adapted to cold temperatures. Plant Cell Environ. **30**(5): 529–538. doi:10.1111/j.1365-3040.2007.01653.x. PMID:17407531.

Han, B., Hughes, D.W., Galau, G.A., Bewley, J.D., and Kermode, A.R. 1997. Changes in late-embryogenesis-abundant (LEA) messenger RNAs and dehydrins during maturation and prema-

ture drying of *Ricinus communis* L. seeds. Planta, **201**(1): 27–35. doi:10.1007/BF01258677. PMID:9004548.

Harauz, G., Ishiyama, N., Hill, C.M.D., Bates, I.R., Libich, D.S., and Farès, C. 2004. Myelin basic protein-diverse conformational states of an intrinsically unstructured protein and its roles in myelin assembly and multiple sclerosis. Micron, **35**(7): 503–542. doi:10.1016/j.micron.2004.04.005. PMID:15219899.

Harwood, J.L. 1980. Plant acyl lipids: structure, distribution, and analysis. *In* Lipids: structure and function. *Edited by* P.K. Stumpf and E.E. Conn. Academic Press, New York. pp. 2–56.

Heyen, B.J., Alsheikh, M.K., Smith, E.A., Torvik, C.F., Seals, D.F., and Randall, S.K. 2002. The calcium-binding activity of a vacuole-associated, dehydrin-like protein is regulated by phosphorylation. Plant Physiol. **130**(2): 675–687. doi:10.1104/pp.002550. PMID:12376635.

Hincha, D.K., Heber, U., and Schmitt, J.M. 1990. Proteins from frost-hardy leaves protect thylakoids against mechanical freeze-thaw damage *in vitro.* Planta, **180**(3): 416–419. ISI:A1990CQ57100015 doi:10.1007/BF01160398.

Hoekstra, F.A., Golovina, E.A., Tetteroo, F.A., and Wolkers, W.F. 2001. Induction of desiccation tolerance in plant somatic embryos: how exclusive is the protective role of sugars? Cryobiology, **43**(2): 140–150. doi:10.1006/cryo.2001.2358. PMID:11846469.

Hundertmark, M., and Hincha, D.K. 2008. LEA (late embryogenesis abundant) proteins and their encoding genes in *Arabidopsis thaliana.* BMC Genomics, **9**(1): 118. doi:10.1186/1471-2164-9-118. PMID:18318901.

Ismail, A.M., Hall, A.E., and Close, T.J. 1999. Purification and partial characterization of a dehydrin involved in chilling tolerance during seedling emergence of cowpea. Plant Physiol. **120**(1): 237–244. doi:10.1104/pp.120.1.237. PMID:10318701.

Jepson, S.G., and Close, T.J. 1995. Purification of a maize dehydrin protein expressed in *Escherichia coli.* Protein Expr. Purif. **6**(5): 632–636. doi:10.1006/prep.1995.1083. PMID:8535156.

Jung, C. 2000. Insight into protein structure and protein-ligand recognition by Fourier transform infrared spectroscopy. J. Mol. Recognit. **13**(6): 325–351. doi:10.1002/1099-1352(200011/12)13:6<325::AID-JMR507>3.0.CO;2-C. PMID:11114067.

Koag, M.C., Fenton, R.D., Wilkens, S., and Close, T.J. 2003. The binding of maize DHN1 to lipid vesicles. Gain of structure and lipid specificity. Plant Physiol. **131**(1): 309–316. doi:10.1104/pp.011171. PMID:12529538.

Koag, M.C., Wilkens, S., Fenton, R.D., Resnik, J., Vo, E., and Close, T.J. 2009. The K-segment of maize DHN1 mediates binding to anionic phospholipid vesicles and concomitant structural changes. Plant Physiol. **150**(3): 1503–1514. doi:10.1104/pp.109.136697. PMID:19439573.

Kosová, K., Vitamvas, P., and Prasil, I.T. 2007. The role of dehydrins in plant response to cold. Biol. Plant. **51**(4): 601–617. ISI:000251185100001 doi:10.1007/s10535-007-0133-6.

Kosová, K., Holková, L., Prásil, I.T., Prásilová, P., Bradácová, M., Vítámvás, P., and Capková, V. 2008. Expression of dehydrin 5 during the development of frost tolerance in barley (*Hordeum vulgare*). J. Plant Physiol. **165**(11): 1142–1151. ISI:000258388300003 doi:10.1016/j.jplph.2007.10.009. PMID:18242771.

Kovacs, D., Kalmar, E., Torok, Z., and Tompa, P. 2008. Chaperone activity of ERD10 and ERD14, two disordered stress-related plant proteins. Plant Physiol. **147**(1): 381–390. doi:10.1104/pp.108.118208. PMID:18359842.

Krimm, S., and Bandekar, J. 1986. Vibrational spectroscopy and conformation of peptides, polypeptides, and proteins. Adv. Protein Chem. **38**(1): 181–364. doi:10.1016/S0065-3233(08)60528-8. PMID:3541539.

Laird, D.J., Mulvihill, M.M., and Lillig, J.A. 2009. Membrane-induced peptide structural changes monitored by infrared and circular dichroism spectroscopy. Biophys. Chem. **145**(2–3): 72–78. doi:10.1016/j.bpc.2009.09.002. PMID:19783088.

Lisse, T., Bartels, D., Kalbitzer, H.R., and Jaenicke, R. 1996. The recombinant dehydrin-like desiccation stress protein from the resurrection plant *Craterostigma plantagineum* displays no defined three-dimensional structure in its native state. Biol. Chem. **377**(9): 555–561. PMID:9067253.

Maruyama, K., Takeda, M., Kidokoro, S., Yamada, K., Sakuma, Y., Urano, K., et al. 2009. Metabolic pathways involved in cold acclimation identified by integrated analysis of metabolites and transcripts regulated by DREB1A and DREB2A. Plant Physiol. **150**(4): 1972–1980. doi:10.1104/pp.109.135327. PMID:19502356.

Mouillon, J.M., Gustafsson, P., and Harryson, P. 2006. Structural investigation of disordered stress proteins. Comparison of full-length dehydrins with isolated peptides of their conserved segments. Plant Physiol. **141**(2): 638–650. doi:10.1104/pp.106.079848. PMID:16565295.

Mouillon, J.M., Eriksson, S.K., and Harryson, P. 2008. Mimicking the plant cell interior under water stress by macromolecular crowding: disordered dehydrin proteins are highly resistant to structural collapse. Plant Physiol. **148**(4): 1925–1937. doi:10.1104/pp.108.124099. PMID:18849483.

New England Biolabs. 2010. IMPACT (Intein-Mediated Purification with an Affinity Chitin-Binding Tag) manual. Available from http://www.neb.com/nebecomm/manualfiles/manualE6950.pdf. New England Biolabs.

Pedras, M.S., and Zheng, Q.A. 2010. Metabolic responses of *Thellungiella halophila/salsuginea* to biotic and abiotic stresses: metabolite profiles and quantitative analyses. Phytochemistry, **71**(5–6): 581–589. doi:10.1016/j.phytochem.2009.12.008. PMID:20122704.

Polverini, E., Fasano, A., Zito, F., Riccio, P., and Cavatorta, P. 1999. Conformation of bovine myelin basic protein purified with bound lipids. Eur. Biophys. J. **28**(4): 351–355. doi:10.1007/s002490050218. PMID:10394626.

Puhakainen, T., Hess, M.W., Mäkelä, P., Svensson, J., Heino, P., and Palva, E.T. 2004. Overexpression of multiple dehydrin genes enhances tolerance to freezing stress in *Arabidopsis.* Plant Mol. Biol. **54**(5): 743–753. doi:10.1023/B:PLAN.0000040903.66496.a4. PMID:15356392.

Rajesh, S., and Manickam, A. 2006. Prediction of functions for two LEA proteins from mung bean. Bioinformation, **1**(4): 133–138. PMID:17597874.

Receveur-Bréchot, V., Bourhis, J.M., Uversky, V.N., Canard, B., and Longhi, S. 2006. Assessing protein disorder and induced folding. Proteins, **62**(1): 24–45. doi:10.1002/prot.20750. PMID:16287116.

Rinne, P.L., Kaikuranta, P.L., van der Plas, L.H., andvan der Schoot, C.. 1999. Dehydrins in cold-acclimated apices of birch (*Betula pubescens* Ehrh.): production, localization and potential role in rescuing enzyme function during dehydration. Planta, **209**(4): 377–388. doi:10.1007/s004250050740. PMID:10550618.

Rorat, T., Szabala, B.M., Grygorowicz, W.J., Wojtowicz, B., Yin, Z., and Rey, P. 2006. Expression of SK3-type dehydrin in transporting organs is associated with cold acclimation in *Solanum* species. Planta, **224**(1): 205–221. doi:10.1007/s00425-005-0200-1. PMID:16404580.

Shimizu, T., Kanamori, Y., Furuki, T., Kikawada, T., Okuda, T., Takahashi, T., et al. 2010. Desiccation-induced structuralization

and glass formation of group 3 late embryogenesis abundant protein model peptides. Biochemistry, **49**(6): 1093–1104. doi:10.1021/bi901745f. PMID:20028138.

Soulages, J.L., Kim, K., Walters, C., and Cushman, J.C. 2002. Temperature-induced extended helix/random coil transitions in a group 1 late embryogenesis-abundant protein from soybean. Plant Physiol. **128**(3): 822–832. doi:10.1104/pp.010521. PMID: 11891239.

Soulages, J.L., Kim, K., Arrese, E.L., Walters, C., and Cushman, J.C. 2003. Conformation of a group 2 late embryogenesis abundant protein from soybean. Evidence of poly (L-proline)-type II structure. Plant Physiol. **131**(3): 963–975. doi:10.1104/pp.015891. PMID:12644649.

Steponkus, P.L., Uemura, M., Joseph, R.A., Gilmour, S.J., and Thomashow, M.F. 1998. Mode of action of the *COR15a* gene on the freezing tolerance of *Arabidopsis thaliana.* Proc. Natl. Acad. Sci. U.S.A. **95**(24): 14570–14575. doi:10.1073/pnas.95.24.14570. PMID:9826741.

Surewicz, W.K., and Mantsch, H.H. 1988. New insight into protein secondary structure from resolution-enhanced infrared spectra. Biochim. Biophys. Acta, **952**(2): 115–130. PMID:3276352.

Surewicz, W.K., Mantsch, H.H., and Chapman, D. 1993. Determination of protein secondary structure by Fourier transform infrared spectroscopy: a critical assessment. Biochemistry, **32**(2): 389–394. doi:10.1021/bi00053a001. PMID:8422346.

Tantos, A., Friedrich, P., and Tompa, P. 2009. Cold stability of intrinsically disordered proteins. FEBS Lett. **583**(2): 465–469. doi:10.1016/j.febslet.2008.12.054. PMID:19121309.

Terzi, E., Hölzemann, G., and Seelig, J. 1997. Interaction of Alzheimer beta-amyloid peptide(1-40) with lipid membranes. Biochemistry, **36**(48): 14845–14852. doi:10.1021/bi971843e. PMID:9398206.

Tolleter, D., Jaquinod, M., Mangavel, C., Passirani, C., Saulnier, P., Manon, S., et al. 2007. Structure and function of a mitochondrial late embryogenesis abundant protein are revealed by desiccation. Plant Cell, **19**(5): 1580–1589. doi:10.1105/tpc.107.050104. PMID:17526751.

Tompa, P., Bánki, P., Bokor, M., Kamasa, P., Kovács, D., Lasanda, G., and Tompa, K. 2006. Protein-water and protein-buffer interactions in the aqueous solution of an intrinsically unstructured plant dehydrin: NMR intensity and DSC aspects. Biophys. J. **91**(6): 2243–2249. doi:10.1529/biophysj.106.084723. PMID: 16798808.

Tunnacliffe, A., and Wise, M.J. 2007. The continuing conundrum of the LEA proteins. Naturwissenschaften, **94**(10): 791–812. doi:10.1007/s00114-007-0254-y. PMID:17479232.

Uversky, V.N., and Dunker, A.K. 2010. Understanding protein nonfolding. Biochim. Biophys. Acta, **1804**(6): 1231–1264. doi:10.1016/j.bbapap.2010.01.017. PMID:20117254.

Vié, V., Van Mau, N., Chaloin, L., Lesniewska, E., Le Grimellec, C., and Heitz, F. 2000. Detection of peptide-lipid interactions in mixed monolayers, using isotherms, atomic force microscopy, and fourier transform infrared analyses. Biophys. J. **78**(2): 846–856. doi:10.1016/S0006-3495(00)76642-2. PMID:10653797.

Wieprecht, T., Apostolov, O., Beyermann, M., and Seelig, J. 1999. Thermodynamics of the alpha-helix-coil transition of amphipathic peptides in a membrane environment: implications for the peptide-membrane binding equilibrium. J. Mol. Biol. **294**(3): 785–794. doi:10.1006/jmbi.1999.3268. PMID:10610796.

Wise, M.J., and Tunnacliffe, A. 2004. POPP the question: what do LEA proteins do? Trends Plant Sci. **9**(1): 13–17. doi:10.1016/j.tplants.2003.10.012. PMID:14729214.

Wolkers, W.F., McCready, S., Brandt, W.F., Lindsey, G.G., and Hoekstra, F.A. 2001. Isolation and characterization of a D-7 LEA protein from pollen that stabilizes glasses *in vitro.* Biochim. Biophys. Acta, **1544**(1-2): 196–206. PMID:11341929.

Wong, C.E., Li, Y., Whitty, B.R., Díaz-Camino, C., Akhter, S.R., Brandle, J.E., et al. 2005. Expressed sequence tags from the Yukon ecotype of *Thellungiella* reveal that gene expression in response to cold, drought and salinity shows little overlap. Plant Mol. Biol. **58**(4): 561–574. doi:10.1007/s11103-005-6163-6. PMID:16021339.

Wong, C.E., Li, Y., Labbe, A., Guevara, D., Nuin, P., Whitty, B., et al. 2006. Transcriptional profiling implicates novel interactions between abiotic stress and hormonal responses in *Thellungiella*, a close relative of *Arabidopsis.* Plant Physiol. **140**(4): 1437–1450. doi:10.1104/pp.105.070508. PMID:16500996.

Xu, J., Zhang, Y.X., Wei, W., Han, L., Guan, Z.Q., Wang, Z., and Chai, T.Y. 2008. BjDHNs confer heavy-metal tolerance in plants. Mol. Biotechnol. **38**(2): 91–98. doi:10.1007/s12033-007-9005-8. PMID:18219589.

Zhang, Y., Li, J., Yu, F., Cong, L., Wang, L., Burkard, G., and Chai, T. 2006. Cloning and expression analysis of SKn-type dehydrin gene from bean in response to heavy metals. Mol. Biotechnol. **32**(3): 205–218. doi:10.1385/MB:32:3:205. PMID: 16632887.

Zhang, C., Ding, Z., Xu, X., Wang, Q., Qin, G., and Tian, S. 2010. Crucial roles of membrane stability and its related proteins in the tolerance of peach fruit to chilling injury. Amino Acids, **39**(1): 181–194 doi:10:1007/s00726-009-0397-6. PMID: 20091071.

Zhu, B., Choi, D.W., Fenton, R., and Close, T.J. 2000. Expression of the barley dehydrin multigene family and the development of freezing tolerance. Mol. Gen. Genet. **264**(1–2): 145–153. doi:10.1007/s004380000299. PMID:11016844.

Appendix A

Appendix A begins on the following page.

Table A1. Analysis of FTIR spectra for secondary structure components of TsDHN-1 bound to large unilamellar lipid vesicles mimicking the plant plasma membrane (PC:PE:PI at 33:47:20), with a lipid-to-protein ratio of 1:1.

Secondary structure components of TsDHN-1	λ_{max} (cm^{-1})	22 °C	17 °C	12 °C	7 °C	2 °C
Side-chain contribution	1613	5±1	6±1	6±1	6±1	6±1
β strand	1632	26±1	27±4	31±3	30±2	30±4
Random coil	1645	30±3	26±2	21±6	21±1	21±2
α helix	1658	18±1	21±1	23±0	25±2	25±5
Turn	1670	13±2	12±2	10±2	10±0	10±2
β strand	1681	5±1	6±2	6±0	4±1	4±0
Side-chain contribution	1693	3±1	2±2	3±1	4±1	4±0

Note: The columns show the percentage area of each peak, with errors representing the standard deviation of two replicates.

Table A2. Analysis of FTIR spectra analysis for secondary structure components of TsDHN-2 bound to large unilamellar lipid vesicles mimicking the plant plasma membrane (PC:PE:PI at 33:47:20), with a lipid-to-protein ratio of 1:1.

Secondary structure components of TsDHN-2	λ_{max} (cm^{-1})	22 °C	17 °C	12 °C	7 °C	2 °C
Side-chain contribution	1612	7±4	12±1	7±5	11±0.5	7±1
β strand	1620	18±2	18±0.5	19±2	21±0.5	29±2
Random coil	1643	38±3	30±2	34±4	22±1	19±3
α helix	1658	28±1	21±1	27±5	25±1	33±1
Turn	1668	5±1	12±3	8±2	9±3	3±1
β strand	1676	6±5	7±5	4±1	9±1	8±5
Side-chain contribution	1691	2±2	2±1	1±2	2±2	1±1

Note: The columns show the percentage area of each peak, with errors representing the standard deviation of two replicates.

Table A3. Analysis of FTIR spectra for secondary structure components of TsDHN-1 bound to large unilamellar lipid vesicles mimicking the plant chloroplast membrane (MGDG:DGDG:SQDG:PC:DMPG:PE:PI at 51:26:7:3:9:1), with a lipid-to-protein ratio of 1:1.

Secondary structure components of TsDHN-1	λ_{max} (cm^{-1})	22 °C	17 °C	12 °C	7 °C	2 °C
Side-chain contribution	1613	12±0	7±2	8±0	10±1	8±2
β strand	1632	32±4	44±2	45±3	44±4	45±3
Random coil	1645	27±4	13±0	10±4	10±0	9±1
α helix	1658	13±4	16±3	19±1	17±3	21±5
Turn	1670	9±0	5±0	8±2	8±0	8±1
β strand	1681	4±4	13±3	6±2	7±0	6±2
Side-chain contribution	1693	3±2	2±1	4±2	3±3	4±2

Note: The columns show the percentage area of each peak, with errors representing the standard deviation of two replicates.

Table A4. Analysis of FTIR spectra for secondary structure components of TsDHN-2 bound to large unilamellar lipid vesicles mimicking the plant chloroplast membrane (MGDG:DGDG:SQDG:PC:DMPG:PE:PI at 51:26:7:3:9:1), with a lipid-to-protein ratio of 1:1.

Secondary structure components of TsDHN-2	λ_{max} (cm^{-1})	22 °C	17 °C	12 °C	7 °C	2 °C
Side-chain contribution	1612	10±1	10±1	9±1	2±1	4±4
β strand	1620	32±1	35±1	33±4	44±1	43±4
Random coil	1643	26±3	25±1	23±2	21±0	18±1
α helix	1658	17±1	18±0	18±1	23±0	22±4
Turn	1668	8±0	6±2	8±0	6±2	5±1
β strand	1676	4±2	4±1	6±1	4±1	4±2
Side-chain contribution	1693	3±2	2±1	3±2	5±3	4±2

Note: The columns show the percentage area of each peak, with errors representing the standard deviation of two replicates.

Table A5. Analysis of FTIR spectra for secondary structure components of TsDHN-1 and TsDHN-2 alone, at the same protein concentrations for samples described in Tables A1–A4.

Components of TsDHN-1	λ_{max}, cm^{-1}	22 °C	5 °C
Side-chain contribution	1615	15	13
β strand	1634	ND	13
Random coil	1642	51	44
α helix	1658	5	2
Turn	1667	29	27
Components of TsDHN-2	**λ_{max}, cm^{-1}**	**22 °C**	**5 °C**
Side-chain contribution	1615	18	14
β strand	1634	ND	11
Random coil	1642	51	46
α helix	1658	7	4
Turn	1667	22	26

Note: The columns show the percentage area of each peak. ND, not detected.

Table A6. Analysis of FTIR spectra for secondary structure components of TsDHN-1 and TsDHN-2 bound to large unilamellar lipid vesicles mimicking the plant plasma membrane (PC:PE:PI at 33:47:20), with a lipid-to-protein ratio of 3:1.

Components of TsDHN-1	λ_{max}, cm^{-1}	22 °C	17 °C	12 °C
Side-chain contribution	1609	10±4	10±1	13±0
β strand	1629	49±2	56±1	57±1
Random coil	1644	12±1	13±1	12±2
α helix	1657	7±0	7±1	7±1
Turn	1665	6±2	5±0	3±0
β strand	1683	6±0	3±0	3±0
Side-chain contribution	1695	10±4	6±1	5±1
Components of TsDHN-2	**λ_{max}, cm^{-1}**	**22 °C**	**17 °C**	**12 °C**
Side-chain contribution	1609	4±1	6±1	7±3
β strand	1629	20±2	19±0	20±1
Random coil	1641	31±1	20±4	14±0
α helix	1648	25±2	30±1	31±5
Turn	1664		12±1	14±2
Turn	1671	12±2	10±2	9±3
β strand	1681	8±0	3±1	5±2

Note: The columns show the percentage area of each peak, with errors representing the standard deviation of two replicates.

Table A7. Analysis of FTIR spectra for secondary structure components of TsDHN-1 and TsDHN-2 bound to large unilamellar lipid vesicles mimicking the plant chloroplast membrane (MGDG:DGDG:SQDG:PC:DMPG:PE:PI at 51:26:7:3:9:1), with a lipid-to-protein ratio of 3:1.

Components of TsDHN-1	λ_{max}, cm^{-1}	22 °C	17 °C	12 °C
Side-chain contribution	1609	13±0	10±2	12±6
β strand	1629	58±0	50±2	56±4
Random coil	1644	17±0	15±1	14±0
α helix	1657	7±2	8±2	6±0
Turn	1665	2±0	6±1	4±0
β strand	1683	1±0	6±1	7±0
Side-chain contribution	1695	2±1	5±1	1±1
Components of TsDHN-2	**λ_{max}, cm^{-1}**	**22 °C**	**17 °C**	**12 °C**
Side-chain contribution	1612	11±2	9±2	11±5
β strand	1624	52±0	55±2	54±1
Random coil	1642	27±0	28±1	10±1
α helix	1648	4±0	6±3	17±1
Turn	1663	6±0	2±0	10±4
Turn	1671	—	—	—

Note: The columns show the percentage area of each peak, with errors representing the standard deviation of two replicates.

Table A8. Analysis of FTIR spectra for secondary structure components of TsDHN-1 and TsDHN-2 bound to large unilamellar lipid vesicles mimicking the plant mitochondrial membrane (PC:PS:PE:Chl at 27:25:29:20), with a lipid-to-protein ratio of 3:1.

Components of TsDHN-1	λ_{max}, cm^{-1}	22 °C	17 °C	12 °C
Side-chain contribution	1609	15±0	7±1	9±0
β strand	1629	49±1	66±1	73±1
Random coil	1644	22±0	15±1	8±2
α helix	1657	2±1	5±1	5±0
Turn	1665	6±0	3±0	3±0
β strand	1683	6±0	2±0	1±2
Side-chain contribution	1695		2±1	2±0
Components of TsDHN-2	**λ_{max}, cm^{-1}**	**22 °C**	**17 °C**	**12 °C**
Side-chain contribution	1609	3±0	5±2	10±5
β strand	1629	17±1	32±4	44±2
Random coil	1641	39±6	17±1	16±5
α helix	1648	24±2	30±3	12±1
Turn	1661	–	–	10±0
Turn	1672	7±1	8±2	3±2
β strand	1679	10±5	8±0	5±0

Note: The columns show the percentage area of each peak, with errors representing the standard deviation of two replicates.